Inorganic Chemistry

Article

pubs.acs.org/IC

Structural Characterization of Magnesium-Based Compounds Mg_9Si_5 and Mg_4Si_3Al (Superconductor) Synthesized under High Pressure and High Temperature Conditions

Shidong Ji,[§,†] Motoharu Imai,[‡] Haikui Zhu,[†] and Shoji Yamanaka*[,†]

[†]Department of Applied Chemistry, Graduate School of Engineering, Hiroshima University, Higashi-Hiroshima 739-8527, Japan

[‡]National Institute for Materials Science, 1-2-1 Sengen, Tsukuba, Ibaraki 305-0047, Japan

Supporting Information

ABSTRACT: Two kinds of magnesium-based compounds Mg_9Si_5 and Mg_4Si_3Al have been prepared under high pressure and high temperature (HPHT) conditions of 5 GPa at 900−1100 °C. Single crystal study revealed that Mg_9Si_5 crystallizes in space group $P6_3$ (No. 173) with the lattice parameters a = 12.411(1) Å, c = 12.345(1) Å, and Z = 6. The structure can be derived from the high pressure form Mg_2Si with the anticotunnite structure; excess Si atoms of Mg_9Si_5 form Si−Si pairs in the prismatic cotunnite columns running along the c axis. Mg_4Si_3Al is obtained by a rapid cooling of a ternary mixture Mg:Al:Si = 1:1:1 from ∼800 °C to room temperature under a pressure of 5 GPa. The compound crystallizes in space group $P4/ncc$ (No. 130) with the lattice parameters a = 6.7225(5) Å, c = 13.5150(9) Å, and Z = 4. The structure consists of an alternate stacking of $[AlSi_2]$ layers having a Cairo pattern and $[Mg_4Si]$ antitetragonal prismatic layers. It can be viewed as composed of hexa-Si-capped tetragonal prismatic cages Mg_8Si_6 with an Al atom at the center of each cage, $Al@Mg_8Si_6$. The compound shows superconductivity with a transition temperature T_c = 5.2 K. The formation regions of the two kinds of new magnesium-based compounds have been proposed.

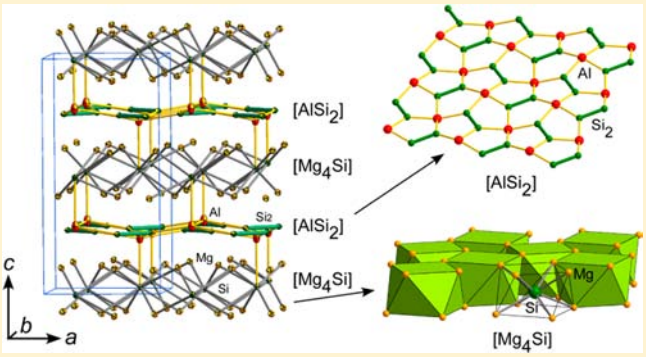

INTRODUCTION

In a previous study we have prepared a new ternary compound $Mg(Mg_{1-x}Al_x)Si$ under high pressure and high temperature (HPHT) conditions of 5 GPa at 1000 °C.[1] It adopts the anticotunnite structure, and shows superconductivity with a transition temperature T_c = 6 K when x > 0.5. A similar ternary compound has been found as fine precipitates by Andersen et al. in an Al-based alloy containing Mg and Si;[2] the precipitates are formed during low temperature aging of the alloy. The formation of the fine coherent precipitates in the Al matrix without boundary is considered to play an important role for the hardening of commercial Al alloys. They also have found several other kinds of Mg−Al−Si ternary and Mg−Si binary compounds as fine precipitates in Al-based alloys.[3,4] Note that no such compounds have been prepared in bulk phases under ambient pressure conditions; Mg_2Si with the antifluorite structure is the only compound known in the ternary system Mg−Al−Si under ambient pressure.[5,6] Recently, it has been reported that Mg_2Si with the antifluorite structure can be transformed to the anticotunnite structure at a high pressure of 7.5−10.4 GPa at room temperature using a diamond anvil cell (DAC).[7,8] The ternary compound $Mg(Mg_{1-x}Al_x)Si$ with the anticotunnite structure, that we have found in a previous study, was also prepared under HPHT condition.[1] It is reasonable to assume that the ternary and binary precipitates found in Al-based alloys are formed under high pressure generated by Al matrix of the alloy.

Since the success of the preparation of the orthorhombic compound $Mg(Mg_{1-x}Al_x)Si$ in the bulk phase under HPHT conditions,[1] we have continued the development of new Mg-based compounds in the Mg−Al−Si ternary system under HPHT conditions, and obtained two kinds of new ternary compounds $Mg_{9-x}Al_xSi_5$ and Mg_4Si_3Al. The former one appears to correspond to the hexagonal phase Mg_9Si_5 found as one of precipitates in Al-based alloy, whose structure was estimated by the study using electron diffraction and energy dispersive X-ray microanalysis coupled with the confirmation by *ab initio* calculation.[3] In this study, we have succeeded in obtaining single crystals suitable for X-ray structural analysis. The second new compound is obtained only in a limited temperature condition by quenching to room temperature under high pressure. The compound has become a superconductor with T_c = 5.2 K. The formation region and the structures of the two compounds are studied in relation with the orthorhombic phase $Mg(Mg_{1-x}Al_x)Si$ reported previously.[1]

Received: December 14, 2012
Published: March 11, 2013

   dx.doi.org/10.1021/ic3027539 | *Inorg. Chem.* 2013, 52, 3953−3961

Table 1. Compositions by EPMA on the Grains Obtained from the Ternary Mixtures with Various Nominal Compositions after HPHT Treatment

			found (at. %)				
nominal composition	thermal protocol[a]	no. marked[b]	Mg	Al	Si	phase[c]	formula
$Mg(Mg_{0.6}Al_{0.4})Si$	S		61.85	2.46	35.69	H	$Mg_{8.66}Al_{0.36}Si_5$
			53.26	13.41	33.33	O	$Mg(Mg_{0.60}Al_{0.40})Si$
$Mg(Mg_{0.5}Al_{0.5})Si$	S		62.64	1.42	35.74	H	$Mg_{8.78}Al_{0.20}Si_5$
			48.93	17.62	33.45	O	$Mg(Mg_{0.60}Al_{0.40})Si$
$Mg(Mg_{0.3}Al_{0.7})Si$	S		62.66	2.03	35.31	H	$Mg_{8.77}Mg_{0.28}Si_5$
			45.73	20.90	33.38	O	$Mg(Mg_{0.37}Al_{0.63})Si$
$Mg_{1.0}Al_{1.0}Si_{1.0}$	Q	1	55.27	7.73	37.10	T	$Mg_{4.43}Al_{0.62}Si_3$
sample I (800 °C)		2	50.57	16.30	33.13	O	$Mg(Mg_{0.51}Al_{0.49})Si$
		3	0.68	59.87	39.45	Al−Si	$Al_{0.60}Si_{0.40}$
$Mg_{1.0}Al_{1.0}Si_{1.0}$	S	4	41.12	25.57	33.31	O	$Mg(Mg_{0.23}Al_{0.77})Si$
sample II (500 °C)		5	0.71	84.50	14.80	Al−Si	$Al_{0.85}Si_{0.15}$

[a]S: The melt was slowly cooled down to 500 °C. Q: The sample was obtained by quenching the mixture from 800 °C. [b]The positions analyzed are marked by the numbers in Figure 5. [c]H: The hexagonal phase. O: The orthorhombic phase. T: The tetragonal phase. Al−Si: Eutectic.

EXPERIMENTAL SECTION

HPHT synthesis was carried out using the Kawai-type multianvil press by the method described in a previous study.[1,9] Typical HPHT conditions were 5 GPa at 950−1000 °C, and the sample was cooled down to room temperature using different thermal protocols. The sample can be quenched to room temperature within a few minutes when the electric power supply is turned off. Single crystal structures were analyzed by using a diffractometer Smart-APEX II (Bruker) as described in a previous paper.[1,10,11] X-ray powder diffraction (XRD) patterns were measured by an imaging plate Guinier diffractometer (Huber 670G) using Mo Kα1 radiation (λ = 0.709 26 Å) with a glass capillary goniometer. Chemical compositions were analyzed by electron probe microanalysis (EPMA) using a wavelength-dispersive X-ray spectrometer (JEOL, JCMA-733) on the samples polished in epoxy resin to avoid topographic effect. Backscattered electron (BSE) images were observed by a scanning electron microscope (Hitachi 3400) for microstructure analysis. Magnetic susceptibility was measured using SQUID-VSM (Quantum Design) under a field of 20 Oe. The *ab initio* calculation of the band structure was performed by the program CASTEP in Accelrys software suit on the structure geometrically optimized as described in a previous study.[12,13]

RESULTS AND DISCUSSION

1. Hexagonal Compound $(Mg_{9-x}Al_x)Si_5$. *1. 1. Preparation.* In a previous study,[1] we have reported that the orthorhombic compound with the anticotunnite structure forms solid solutions in a wide composition range $Mg(Mg_{1-x}Al_x)Si$ ($0.3 < x < 0.8$), and is always associated with a hexagonal phase and sometimes with eutectic Si−Al. This is due to the fact that the orthorhombic compound peritectically decomposes to the hexagonal phase at a temperature around 900 °C. The hexagonal phase appears to be identical to the β' phase found as fine precipitates in an Al-based alloy during precipitation hardening. Vissers et al. analyzed the β' phase precipitates with a rod shape of ~10 nm in diameter and several hundred nanometers long using electron diffraction technique and energy dispersive composition microanalysis (EDX).[3] The composition was determined to be Mg_9Si_5, and the structure was tentatively assigned to have space group $P6_3/m$ and the lattice parameters a = 7.15 Å and c = 12.15 Å. Since the structure was estimated from a limited number of diffraction data using a tiny single crystal under an electron microscope, the obtained structure was confirmed by means of *ab initio* calculation.

In a previous study, we have found that the ternary compound $Mg(Mg_{1-x}Al_x)Si$ with the anticotunnite structure obtained under HPHT conditions undergoes a peritectic decomposition to a mixture of a hexagonal phase plus an Al−Si eutectic around 800 °C.[1] We assumed that the hexagonal phase should have a structure proposed by Vissers et al. on the basis of β' phase precipitates.[3] In this study, we have found the single crystals of the hexagonal phase suitable for X-ray structural study. We have also analyzed the compositions of the orthorhombic (anticotunnite $Mg(Mg_{1-x}Al_x)Si$) as well as the hexagonal phases using EPMA on the samples obtained from the ternary mixtures with various nominal compositions $Mg(Mg_{1-x}Al_x)Si$ ($0.3 < x < 0.8$) by HPHT treatment at 5 GPa and 1000 °C, followed by slow cooling to room temperature in 5 h. We have found the following results: (a) There are two kinds of ternary grains with the Si contents close to 33.3 and 35.7 at. % (atomic %) as shown in Table 1. (b) The grains with the silicon content close of 33.3 at. % are the orthorhombic phase, and have various Mg/Al ratios in a range $Mg(Mg_{1-x}Al_x)Si$ ($0.3 < x < 0.8$) as previously reported for the orthorhombic phase. (c) The grains with the silicon content close of 35.7 at. % are the hexagonal phase. In contrast to the variable ternary composition of the orthorhombic phase, the hexagonal phase has a narrow composition range $Mg_{9-x}Al_xSi_5$ ($0.2 < x < 0.4$), very similar to the binary Mg_9Si_5 reported for the β' phase by Vissers et al.[3] (d) It should be noted that we had observed only two kinds of grains with silicon contents of 33.3 and 35.7 at. % against varying Mg/Al ratios (Table 1). This implies that the silicon sites are not subjected to substitution by Al, but only the Mg sites are substituted by Al.

In order to obtain the binary single crystals of the hexagonal phase, an element mixture with an atomic ratio Mg:Si = 9: 5 was treated under 5 GPa at 1100 °C for 0.5 h, and then cooled down to 800 °C in 2 h, followed by quenching to room temperature. Single crystals were obtained, and EPMA study confirmed that the nominal composition was maintained at Mg_9Si_5 of the hexagonal phase. (Found: Mg 61.3, Si 38.7 wt %. Calcd for Mg_9Si_5: Mg 60.9, Si 39.1 wt %.) The hexagonal phase is hereafter called $(Mg_9Si_5)_{HP}$. We have also treated mixtures with the atomic ratios of Mg/Si = 2/1 and 1/1 in a similar way at 1000 °C under 5 GPa. The former mixture produced a mixture of $(Mg_9Si_5)_{HP}$ and Mg, while the latter one is a mixture of $(Mg_9Si_5)_{HP}$ and Si. $(Mg_9Si_5)_{HP}$ appears to melt at temperatures above 1000 °C under high pressure, close to

dx.doi.org/10.1021/ic3027539 | Inorg. Chem. 2013, 52, 3953−3961

the melting temperature of 1084 °C for Mg_2Si under ambient pressure.[14] The hexagonal $(Mg_9Si_5)_{HP}$ was thermally treated at 450 °C in an h-BN cell for 20 min under an Ar atmosphere, and the XRD powder pattern was measured. The compound was found to be changed into the ambient phase Mg_2Si with the antifluorite strucuture and a small amount of Si, showing that $(Mg_9Si_5)_{HP}$ is a quenchable high pressure phase.

1. 2. Single Crystal Characterization of Mg_9Si_5. The crystal structure was analyzed on $(Mg_9Si_5)_{HP}$ single crystals obtained from a binary mixture Mg_9Si_5 by HPHT treatment, and the results are summarized in Tables 2 and 3. The compound

Table 2. Details of the Crystal Structure Investigations for Mg_9Si_5 and Mg_4AlSi_3

	Mg_9Si_5	Mg_4AlSi_3
fw	359.24	208.49
cryst size (mm^3)	0.1 × 0.1 × 0.1	0.13 × 0.1 × 0.1
space group	$P6_3$ (No. 173)	$P4/ncc$ (No. 130)
R_{int}	0.0235	0.0654
a (Å)	12.411(1)	6.7225(5)
b (Å)	12.411(1)	6.7225(5)
c (Å)	12.345(1)	13.5150(9)
α, β, γ (deg)	90, 90, 120	90, 90, 90
V (Å^3), Z	1646.8(2), 6	610.77(8), 4
d_{calcd} (g/cm^3)	2.173	2.267
T (K)	293	293
λ Mo Kα (Å)	0.710 73	0.710 73
μ mm^{-1}	1.106	1.191
abs corr	empirical	numerical
$F(000)$	1068	412
θ_{max} (deg)	29.04	27.4
index ranges	$-16<h<16$, $-16<k<16$, $-16<l<16$	$-8<h<8$, $-8<k<8$, $-17<l<17$
refln nos.	19 989	3608
total reflns	1502	357
obsd [$I \geq 2\sigma(I)$]	1324	310
no. variables	132	21
GOF on F_o^2	1.134	1.143
R1/wR2 [$I \geq 2\sigma(I)$]	0.0149/0.0345	0.031/0.0687
R1/wR2 (all data)	0.0198/0.0364	0.0414/0.0728
largest diff peak and hole (e$^-$/Å^3)	0.248/−0.212	0.722/−0.648

crystallizes in an acentric space group $P6_3$ with the lattice parameters a = 12.411(1) Å and c = 12.345(1) Å. The β' phase found as precipitates in Al-based alloy $(Mg_9Si_5)_{\beta'}$ had a slightly smaller unit cell and a higher pseudosymmetry of $P6_3/m$.[3] The two kinds of the hexagonal unit cells $(Mg_9Si_5)_{HP}$ and $(Mg_9Si_5)_{\beta'}$ are compared in Table 4 and Figure 1, together with the lattice parameters of the orthorhombic $(Mg_{2-x}Al_xSi)_{ortho}$ with the anticotunnite ($PbCl_2$) structure. The unit cell used in the analysis of the β' phase in Al alloy was $1/3\ (1/\sqrt{3} \times 1/\sqrt{3})$ of the present cell $(Mg_9Si_5)_{HP}$ with a slightly smaller c parameter. The two structures appear to be basically the same. The β' phase has an averaged structure; $(Mg_9Si_5)_{HP}$ has a superstructure of the β' phase in the ab plane. Note that $(Mg_{2-x}Al_xSi)_{ortho}$ can have a pseudohexagonal cell with the relations a_{ortho} = 6.9242(2) Å $\approx \sqrt{3}/2\ c_{orth} \approx a_{\beta'}$, and $b_{orth} \approx 1/3\ c_{\beta'}$. As shown in Figure 2, in $(Mg_{2-x}Al_xSi)_{ortho}$, each Si atom is coordinated by 9 (Mg, Al) atoms, forming a three capped trigonal prism polyhedron. Such polyhedra are aligned along the b direction sharing top and base triangles, forming anticotunnite columns. Figure 3 shows the structure of $(Mg_9Si_5)_{HP}$. The unit cell of $(Mg_9Si_5)_{HP}$ contains 9 such columns running along the c direction, 6 of which are normal ones with three Si atoms arranged along the c direction in the column of the unit cell length as shown in Figure 3. The remaining 3 columns contain 4 silicon atoms for each forming two Si−Si pairs. This is the reason that the $(Mg_9Si_5)_{HP}$ has a higher Si content than $(Mg_{2-x}Al_xSi)_{ortho}$ with the anticotunnite structure. As shown in Table 1, the Mg sites are subjected to substitution by Al within a limited range of x in the ternary phase $Mg_{9-x}Al_xSi_5$ ($x < 0.4$).

Germanide and stannide analogues Mg_2B_{1+x} (B = Ge, Sn) have been prepared using a similar high pressure conditions by Bolotina et al.[15] Those compounds also have similar hexagonal structures like $(Mg_9Si_5)_{HP}$. However, the two types of anticotunnite columns with three or four B atoms in the column are arranged in an incommensurate manner along the c direction with each other.

In the structural analysis of $(Mg_9Si_5)_{HP}$, an excess of positive electron density of 1.4 e/Å^3 was observed at a position near Si1 site (Table 3), and the structure was refined using disorder; 85% Si1 atoms were estimated to be disordered with 15% of Si11 atoms separated by 0.9 Å along the c direction. The introduction of this disorder reduced the Fourier residue to +0.248 e/Å^3 as shown in Table 2.

2. Tetragonal Compound Mg_4AlSi_3. *2.1. Preparation.* As described in the preparation of the hexagonal compound $(Mg_9Si_5)_{HP}$, we have treated ternary mixtures with various nominal compositions $Mg_{2-x}Al_xSi$ ($0.3 < x < 0.8$) under HPHT conditions along the line shown in the ternary phase diagram of Figure 4. When the mixtures were quenched from 1000 °C, the hexagonal phase was obtained as a major phase with the orthorhombic phase plus Al−Si. This finding implies that a large primary field of the hexagonal phase extends over the ternary phase diagram as shown in Figure 4. However, when the x value increased up to 1, whose composition is marked by "T" in the ternary phase diagram, we had a very different product by quenching. The detailed thermal protocol used under a pressure of 5 GPa was the following: a ternary mixture with a nominal composition $Mg_{1.0}Al_{1.0}Si_{1.0}$ was heated up to 1050 °C. After being kept for 1 h at the temperature, the mixture was cooled down to 800 °C in 20 min, followed by quenching to room temperature under the pressure. This sample is called sample I (800 °C). Another separate sample with the same ternary composition $Mg_{1.0}Al_{1.0}Si_{1.0}$ was also heated at 1050 °C for 1 h under the same pressure, and then slowly cooled down to 500 °C in 3 h, followed by cooling to room temperature. This sample is called sample II (500 °C). The BSE images and the EPMA chemical compositions of the two samples are compared in Figure 5 and Table 1. In sample II (500 °C) obtained after the slow cooling to 500 °C, the grains containing 33.3 at. % Si, i.e., $(Mg_{2-x}Al_xSi)_{ortho}$, are well grown, and surrounded by Al−Si eutectic. On the contrary, in sample I (800 °C) obtained by quenching the ternary mixture from a higher temperature of 800 °C, two kinds of grains with 33.3 and 37.1 at. % Si are observed. These are called grain (33.3 at. % Si) and grain (37.1 at. % Si) hereafter. The shapes of the two kinds of grains with the different Si contents are quite different, although the sizes are in a similar range. Note that grain (37.1 at. % Si) has a clear grain edge surrounded by Al−Si eutectic, whereas grain (33.3 at. % Si) has diffuse grain boundaries, and seemed to be an aggregate of smaller diffuse grains. Grain (33.3 at. % Si) is the orthorhombic phase $(Mg_{2-x}Al_xSi)_{ortho}$, which is

dx.doi.org/10.1021/ic3027539 | Inorg. Chem. 2013, 52, 3953−3961

Table 3. Atomic Coordinates and Equivalent Displacement Parameters for Mg_9Si_5

atom	position	occupancy	x	y	z	U_{eq}, Å^2
Si1	2a	0.84	0	0	0.0436(2)	0.0122(6)
Si11	2a	0.16	0	0	−0.0338(16)	0.039(5)
Si2	2a	1	0	0	0.249 26(15)	0.0155(2)
Si3	6c	1	0.331 01(3)	0.003 68(3)	0.255 63(12)	0.009 36(10)
Si4	2b	1	1/3	2/3	−0.095 12(12)	0.0153(3)
Si5	6c	1	0.336 33(6)	0.335 37(6)	0.419 53(9)	0.0094(3)
Si6	6c	1	0.335 80(7)	0.335 86(7)	0.089 64(10)	0.0098(2)
Si7	2b	1	1/3	2/3	0.108 00(13)	0.0153(3)
Si8	2b	1	2/3	1/3	−0.097 07(12)	0.0147(3)
Si9	2b	1	2/3	1/3	0.105 76(13)	0.0151(3)
Mg1	6c	1	0.243 37(5)	0.169 83(5)	0.2526(1)	0.012 20(12)
Mg2	6c	1	0.533 56(4)	0.404 69(4)	0.254 16(9)	0.015 10(11)
Mg3	6c	1	0.077 34(9)	0.233 16(14)	0.093 98(6)	0.0161(2)
Mg4	6c	1	0.827 06(11)	0.252 80(9)	0.079 34(7)	0.0129(2)
Mg5	6c	1	0.498 22(10)	0.589 45(9)	0.090 15(7)	0.0128(2)
Mg6	6c	1	0.265 60(5)	0.456 60(5)	0.255 81(10)	0.015 28(11)
Mg7	6c	1	0.253 91(10)	0.425 93(11)	−0.073 03(7)	0.0128(2)
Mg8	6c	1	0.499 59(11)	0.4089(1)	−0.081 12(6)	0.0128(2)
Mg9	6c	1	0.072 11(10)	0.213 22(14)	0.414 14(6)	0.0183(2)

Table 4. Lattice Parameters and Pseudosymmetry among $(Mg_{2-x}Al_xSi)_{ortho}$, $(Mg_9Si_5)_{\beta'}$, and $(Mg_9Si_5)_{HP}$

formula	$(Mg_{2-x}Al_xSi)_{ortho}$ anticotunnite structure[a]	$(Mg_9Si_5)_{\beta'}$ precipitate in Al alloy[b]	$(Mg_9Si_5)_{HP}$[c]
space group	*Pnma* (No. 62)	$P6_3/m$ (No. 176)	$P6_3$ (No. 173)
Z	4	2	6
lattice params, Å	a_{orth} = 6.9242(2) ≈ $\sqrt{3}/2\ c_{orth}$	$a_{\beta'}$ = 7.15 ≈ c_{orth}	$a_{hex} = \sqrt{3}a_{\beta'}$ = 12.411(1)
	c_{orth} = 7.9618(2)		
	b_{orth} = 4.1380(1)	$c_{\beta'} = 3b_{orth}$ ≈ 12.15	$c_{hex} \approx c_{\beta'} = 3b_{orth}$ ≈ 12.345(1)
V, Å^3	228.12(1)	537.9	1646.8(2)

[a]ref 1 [b]ref 3 [c]This study.

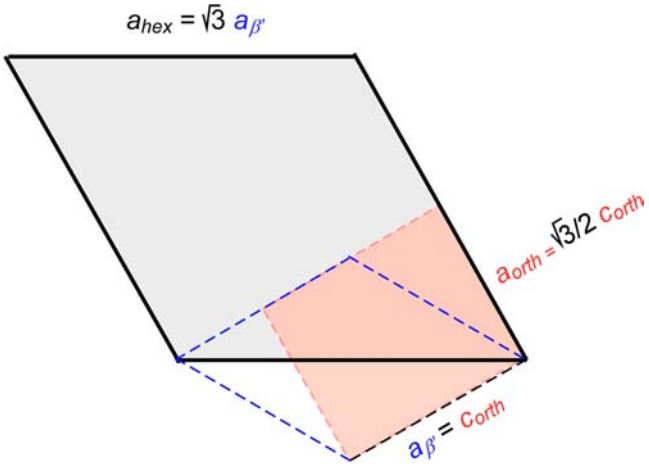

Figure 1. Lattice parameters and pseudosymmetry in the *ab* planes of $(Mg_{2-x}Al_xSi)_{ortho}$ (dashed red line), $(Mg_9Si_5)_{\beta'}$ (black line), and $(Mg_9Si_5)_{HP}$ (dashed blue line).

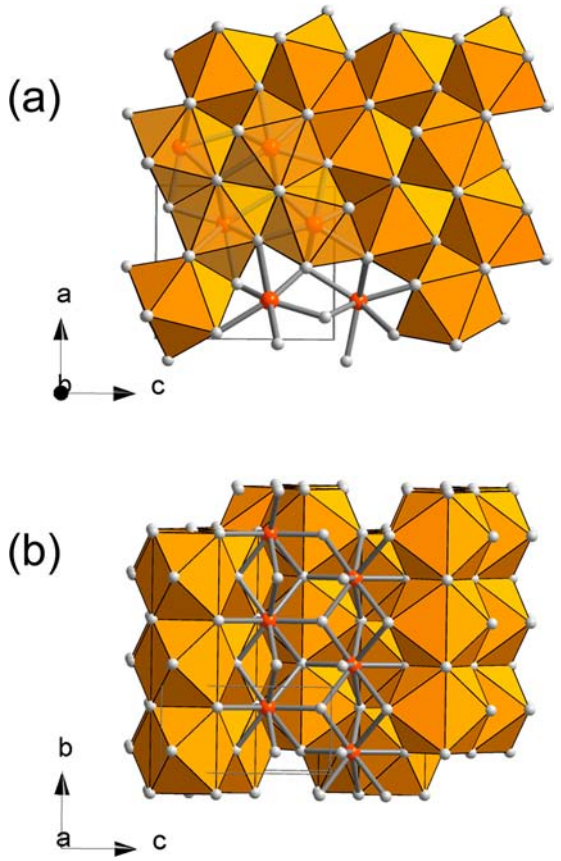

Figure 2. Schematic illustration of the structure of the orthorhombic $Mg_{2-x}Al_xSi$ with the anticotunnite structure showing the cotunnite columns running along the *b* direction: (a) the view along the *b* axis, and (b) the view along the *a* axis. Si atoms (red balls) are 9-coordinated by Mg + Al atoms (white balls).

formed during the slow cooling as mentioned above. The BSE image of Figure 5 suggests that the orthorhombic phase is going to be formed by the reaction of grain (37.1 at. % Si) with Al−Si eutectic during annealing, and grows during slow cooling to 500 °C. This reaction appears to have already started at temperatures above 800 °C, when sample I (800 °C) was quenched to room temperature.

As shown in Table 1, the Si content in grain (37.1 at. % Si) is different from those of the hexagonal and the orthorhombic phases. It must be a new compound. As shown later, we could

dx.doi.org/10.1021/ic3027539 | *Inorg. Chem.* 2013, 52, 3953−3961

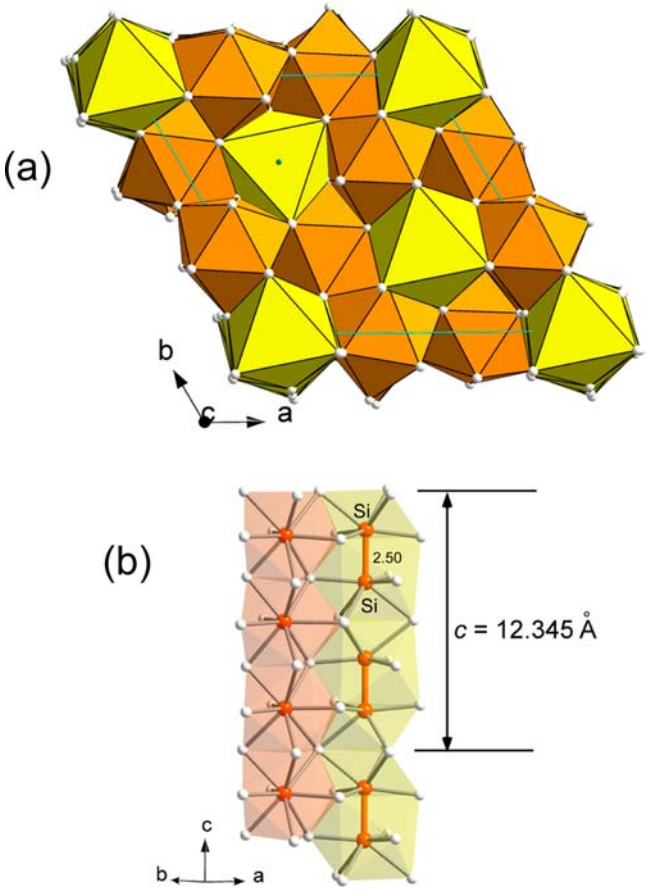

Figure 3. Schematic illustration of the structure of $(Mg_9Si_5)_{HP}$ showing the two types of cotunnite columns running along the *c* direction: (a) the view along the *c* direction, and (b) the view along the direction parallel to the *ab* plane. The brown columns (6 columns per unit cell) are normal ones similar to those shown in Figure 2. The yellow columns (3 columns per unit cell) have 4 silicon atoms (red balls) in each one with a unit cell length (12.345 Å), forming two Si–Si pairs with a bond distance 2.50 Å. Mg atoms are shown by white balls.

pick up single crystals of this compound from sample I (800 °C), and the structural analysis revealed that the compound has a tetragonal unit cell, and a composition $Mg_4(Mg_{1-x}Al_x)Si_3$, with the calculated Si content being 37.5 at. %.

2.2. Phase Diagram. We have tried to obtain the tetragonal compound as a single phase, and treated several kinds of mixtures with nominal compositions $Mg_4(Mg_{1-x}Al_x)Si_3$ ($0 < x < 1$) along the line shown in the ternary phase diagram of Figure 4, parallel with the line of the solid solutions for the orthorhombic phase $(Mg_{2-x}Al_xSi)_{ortho}$. The mixtures were heated at 1100 °C for 1 h under a pressure of 5 GPa, and cooled down slowly to 500 °C during 3 h. The products were found to be a mixture of the orthorhombic and the hexagonal phases. A small amount of tetragonal phase was obtained when the mixtures were quenched from 1000 °C; however, the amount was much smaller compared with that found in sample I (800 °C). These findings suggest that the tetragonal phase can exist in a very narrow temperature range under high pressure.

A schematic image of the phase diagram showing the formation region of the tetragonal phase is proposed in Figure 6. Although it is difficult to present the ternary system in a pseudobinary diagram, this diagram shows a cross section of the ternary phase diagram along a line parallel to $Mg_4(Mg_{1-x}Al_x)Si_3$

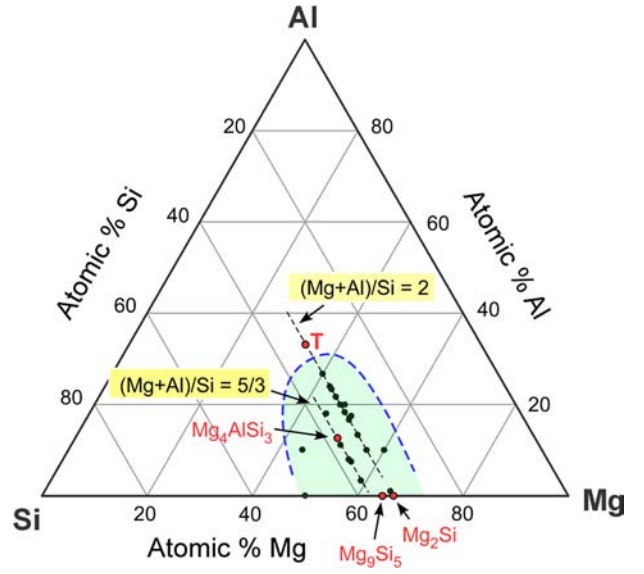

Figure 4. Mg–Al–Si ternary phase diagram having a large Mg_9Si_5 primary field (shadowed by blue). Ternary mixtures with two series of nominal compositions $Mg_{2-x}Al_xSi$ and $Mg_{5-x}Al_xSi_3$ have been treated under HPHT conditions. A ternary mixture with a composition $Mg_{1.0}Al_{1.0}Si_{1.0}$ is marked by "T" at the center of the diagram.

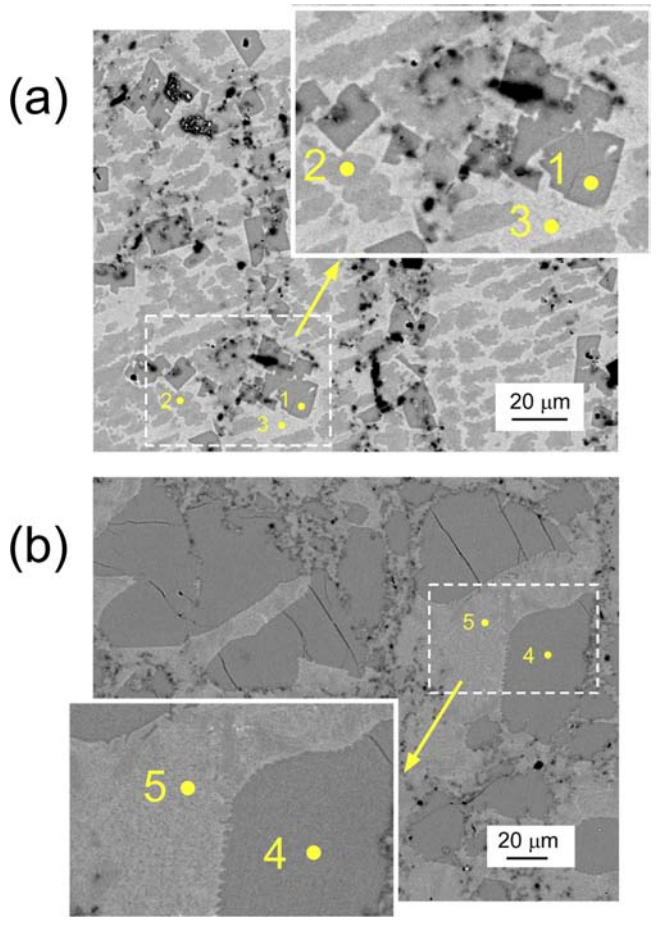

Figure 5. BSE images of (a) sample I (800 °C) and (b) sample II (500 °C). The compositions marked by numbers 1–5 are given in Table 1.

and $Mg_{2-x}Al_xSi$ lines, expressing the large primary field of the hexagonal phase and a narrow formation region of the

dx.doi.org/10.1021/ic3027539 | Inorg. Chem. 2013, 52, 3953–3961

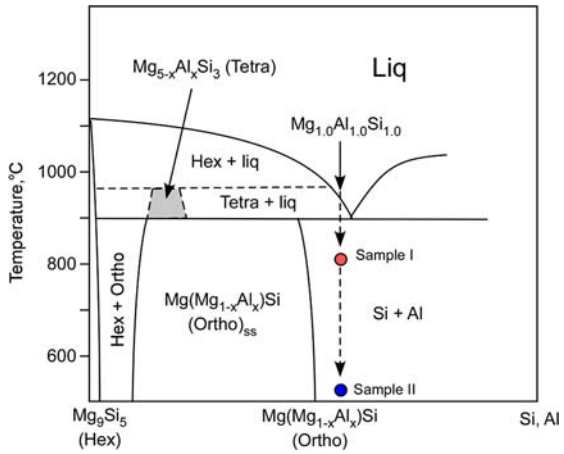

Figure 6. Pseudobinary phase diagram showing the formation region of Mg_4AlSi_3 from a mixture $Mg_{1.0}Al_{1.0}Si_{1.0}$. The primary field of the hexagonal phase extends over a wide compositional area.

tetragonal phase. Note that the starting composition ($Mg_{1.0}Al_{1.0}Si_{1.0}$) of the ternary mixture for the preparation of sample I (800 °C) was very far from the composition of the tetragonal phase. It is likely that the melt of this composition can directly cross the liquidus line for the precipitation of the tetragonal phase as shown in Figure 6. The tetragonal phase can be grown during slow cooling in the narrow temperature range ~950−850 °C. Sample I (800 °C) was obtained by cooling the melt from 1050 to 800 °C in 20 min. If the mixture is annealed for much longer time below the decomposition temperature around ~900 °C, it is converted to the orthorhombic phase as shown in the BSE image of Figure 5.

Sample II (500 °C) with the well grown orthorhombic phase was obtained by cooling down the melt slowly to 500 °C in 3 h. The temperature scale of Figure 6 was estimated from the findings described above. It is considered to be within an error of about 50 °C. Sample I (800 °C) containing a mixture of the tetragonal and the orthorhombic phases was thermally treated at 500 °C for 20 min in an h-BN cell under Ar atmosphere. The XRD measurement revealed that the mixture of the two phases was decomposed to a mixture of Mg_2Si with the antifluorite structure (ambient pressure phase) and an Al−Si eutectic. It is evident that the two kinds of compounds are high pressure phases, and quenchable to ambient pressure condition.

2.3. Single Crystal Characterization. The composition of the single crystals of the tetragonal phase obtained from sample I (800 °C) was determined to be $Mg_4(Mg_{1-x}Al_x)Si_3$ ($x \sim 0.6$) (Table 3) by EPMA. The single crystal analysis results are summarized in Tables 2 and 5. It crystallizes in space group *P*4/*ncc* (No. 130) with the lattice parameters $a = 6.7225(5)$ Å, $c = 13.5150(9)$ Å, and $Z = 4$. The schematic structural model for $Mg_4(Mg_{1-x}Al_x)Si_3$ is shown in Figure 7. The EPMA composition indicates that the Al site is partially substituted by Mg. Although Si and Al atoms cannot be distinguished by X-ray analysis, the atoms bonded at the shortest distance (2.43 Å) were attributed to Si atoms, forming Si−Si pairs. The rest of Si atoms are tentatively placed at the center of Mg antitetragonal prism polyhedra; the bond distances 2.800 Å (4 Si−Mg) and 2.866 Å (4 Si−Mg) are slightly longer than 2.750 Å in the ambient phase Mg_2Si with the antifluorite structure, where Mg atoms form tetragonal prism polyhedra surrounding Si atoms.[6] The structure can be viewed as composed of alternate stacking of the two types of layers, $[AlSi_2]$ and $[Mg_4Si]$. The layer $[AlSi_2]$ forms a Cairo pattern, in which four Si−Si pairs are bonded with an Al atom in almost coplanar planes. This pattern is found in the binary U_3Si_2 and the ternary silicides Y_2LiSi_2 and Nd_2ScSi_2 with the Si−Si distances being 2.40, 2.35, and 2.44 Å, respectively,[16,17] close to 2.35 Å in the element, and comparable with the bond distance (2.43 Å) found in the Cairo pattern $[AlSi_2]$ of this study. The tetragonal U_3Si_2 or Zr_3Al_2 type structure contains hundreds of isotypic compounds with the characteristic Cairo pattern.[18]

The $[Mg_4Si]$ layers consist of edge-shared Mg_8Si polyhedra with an antitetragonal prism coordination. The Al atoms of the Cairo pattern $[AlSi_2]$, and the Si atoms in the $[Mg_4Si]$ layers are linked along the *c*-direction. At the same time, the Si atoms in the Cairo pattern are coordinated by Mg atoms of $[Mg_4Si]$ layers. When we focus on the polyhedron Mg_8Si_6 surrounding an Al atom of the Cairo pattern, $Al@Mg_8Si_6$ (Figure 8a), it is a hexa-Si-capped tetragonal prismlike clathrate. The Si capped tetragonal prisms are linked by Si−Si pairs and face sharing as shown in Figure 8.

3. Superconductivity. The orthorhombic phase is a superconductor with T_c ~6 K as reported previously.[1] The tetragonal phase is always associated with the orthorhombic phase. As described above, it is difficult to obtain the tetragonal compound as single phase. In order to measure the magnetic susceptibility of the tetragonal phase alone, some single crystals were selected by a single crystal X-ray diffractometer (Bruker Smart-APEX II). Figure 9 shows the temperature dependence of the magnetic susceptibility of about 0.01 mg of the selected crystals measured by a SQUID magnetometer. It is evident that the tetragonal phase is also a superconductor with $T_c = 5.2$ K. The volume fraction was estimated to be larger than 60%.

We have reported that the orthorhombic phase $Mg(Mg_{1-x}Al_x)Si$ showed superconductivity when $x > 0.5$.[1] The hexagonal phase did not become a superconductor down to 1.9 K, although it has a structure similar to the orthorhombic phase with the anticotunnite structure. The hexagonal phase has a limited solubility range for Al with $x < 0.4$ in $Mg_{9-x}Al_xSi_5$. The low solubility of Al would be the reason that the hexagonal phase does not show superconductivity.

4. *Ab Initio* Calculation. The electron density of states (DOS) of the tetragonal phase with a stoichiometric composition Mg_4AlSi_3 was calculated using CASTEP software. The calculation conditions are the same as that used for the orthorhombic phase.[1] The results are shown in Figure 10. The Mulliken charges were calculated to be Si1, −0.92; Si2, −0.70;

Table 5. Atomic Coordinates and Equivalent Displacement Parameters for Mg_4AlSi_3

atom	position	*x*	*y*	*z*	U_{eq}, Å^2
Si1	4c	1/4	1/4	0.4888(1)	0.0125(4)
Si2	8f	0.1222(1)	−0.1222(1)	1/4	0.0145(3)
Al	4c	1/4	1/4	0.2811(2)	0.0247(5)
Mg	16g	−0.0952(2)	0.0694(2)	0.4027(1)	0.0160(3)

dx.doi.org/10.1021/ic3027539 | *Inorg. Chem.* 2013, 52, 3953−3961

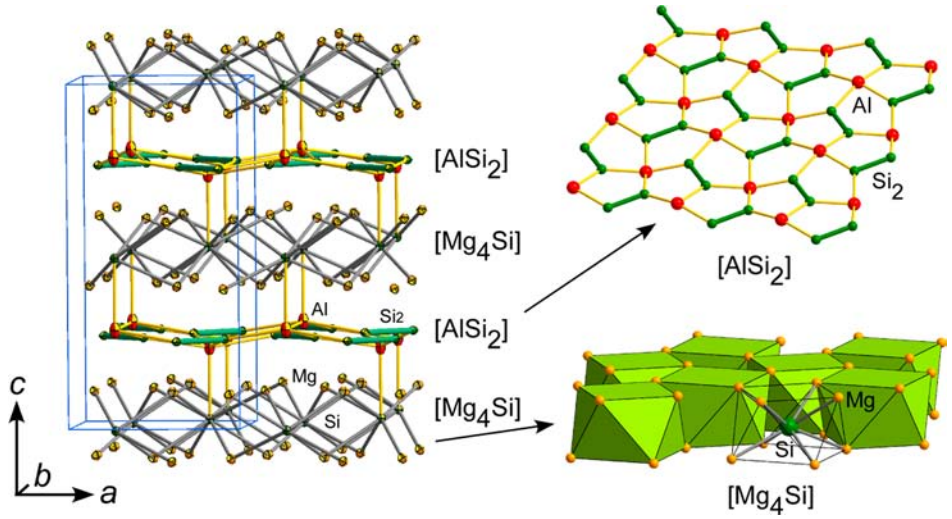

Figure 7. Structure of Mg_4AlSi_3 composed of alternate stacking of $[Mg_4Si]$ and $[AlSi_2]$ layers. The $[AlSi_2]$ layers form an almost coplanar Cairo pattern with a short Si−Si bond distance (2.43 Å). The $[Mg_4Si]$ layers consist of Mg antitetragonal prism polyhedra surrounding Si atoms.

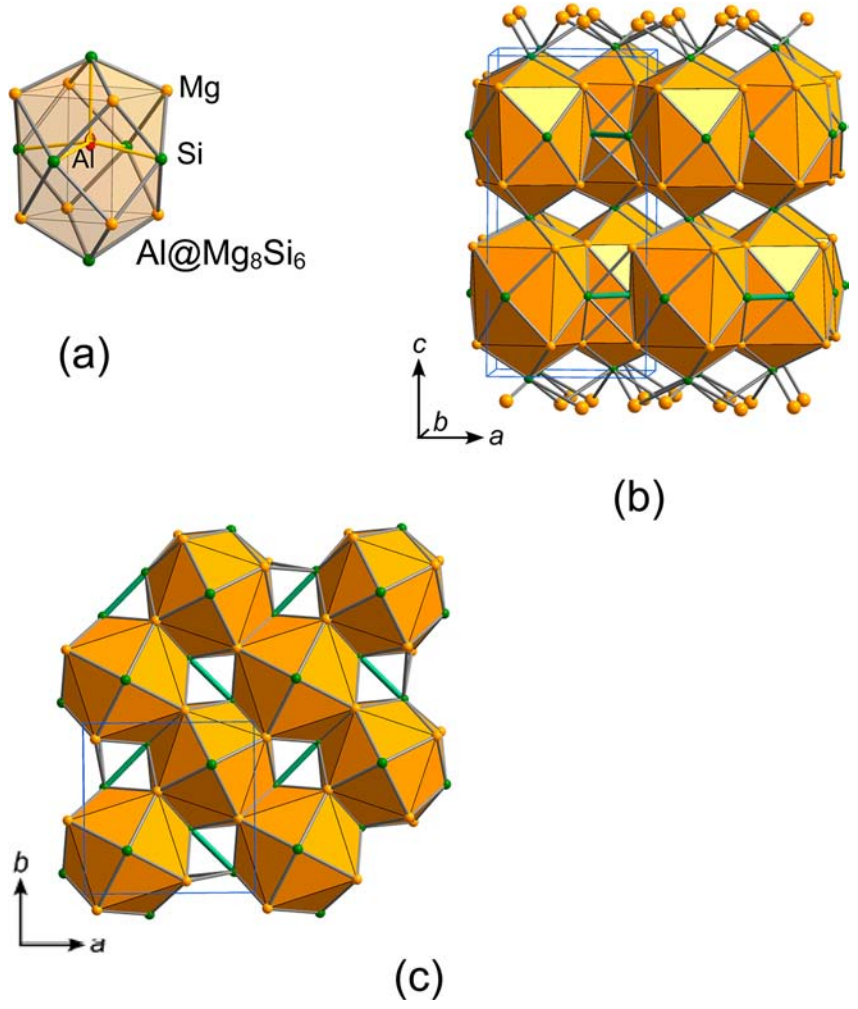

Figure 8. Schematic illustration of the structure of Mg_4AlSi_3 emphasizing the $Al@Mg_8Si_6$ polyhedral cages (a) linked by face sharing and Si−Si bonds in the Cairo pattern: (b) side view and (c) top view along the *c* direction.

Al, −0.09; and Mg, 0.60 e.[19−21] Therefore the alternate layers have charges $[AlSi_2]^{-1.48}$ and $[Mg_4Si]^{+1.48}$. The two kinds of oppositely charged layers are alternatively stacked along the *c* direction. As shown by the partial DOS profile, the Mg 2p orbitals have a large contribution to the total DOS near the Fermi level. The superconductivity appears to occur in the $[Mg_4Si]$ layers. However, a large DOS is not a sufficient

dx.doi.org/10.1021/ic3027539 | *Inorg. Chem.* 2013, 52, 3953−3961

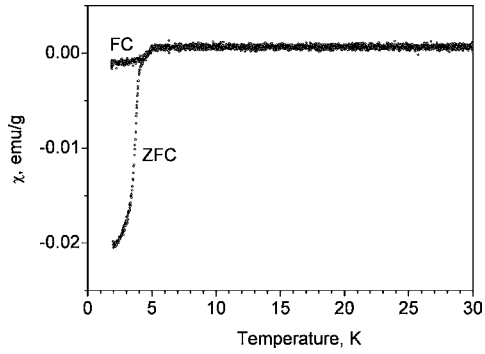

Figure 9. Temperature dependence of the magnetic susceptibility of ~0.01 mg of Mg_4AlSi_3 single crystals under a magnetic field of 20 Oe: ZFC, zero field cooling; and FC, field cooling mode. A superconducting transition was observed at 5.2 K.

condition for superconductivity. For more detailed discussion, theoretical study is needed.

CONCLUSIONS

We have found two kinds of new magnesium-based compounds $Mg_{9-x}Al_xSi_5$ (space group $P6_3$) and Mg_4AlSi_3 (space group $P4/ncc$). Single crystal studies have revealed that the hexagonal compound has a very similar structure as the precipitates found in Al alloy, implying that the precipitates should be formed under a high pressure condition generated in Al alloy matrix. The compound congruently melts, and has a very limited solubility range of Al with $x < 0.4$ in $Mg_{9-x}Al_xSi_5$. The tetragonal phase is obtained only in a limited temperature range and a quenched condition under high pressure. The structure is composed of the alternate stacking of $[AlSi_2]$ and $[Mg_4Si]$ layers; the $[AlSi_2]$ layers form a Cairo pattern, and the $[Mg_4Si]$ layers consist of edge shared Mg antitetragonal prism polyhedra surrounding Si atoms. The compound shows superconductivity with $T_c = 5.2$ K. It is interesting to note that the two kinds of high pressure phases contain Si−Si pairs in the structures with the bond distances 2.50 and 2.43 Å, comparable with the Si−Si distance in the elemental Si of the diamond structure.

ASSOCIATED CONTENT

Supporting Information

CIF data for Mg_9Si_5 and Mg_4AlSi_3. This material is available free of charge via the Internet at http://pubs.acs.org.

AUTHOR INFORMATION

Corresponding Author

*E-mail: syamana@hiroshima-u.ac.jp.

Present Address

[§]Shanghai Institute of Ceramics (SIC), Chinese Academy of Sciences (CAS), Dingxi 1295, Shanghai 200050, China.

Notes

The authors declare no competing financial interest.

ACKNOWLEDGMENTS

This work has been supported by the Japan Society for the Promotion of Science (JSPS) through its "Funding Program for World-Leading Innovative R&D on Science and Technology (FIRST) Program".

REFERENCES

(1) Ji, S.-D.; Tanaka, M.; Zhang, S.; Yamanaka, S. *Inorg. Chem.* **2012**, *51*, 10300−10305.

(2) Andersen, S. J.; Marioara, C. D.; Froseth, A.; Vissers, R.; Zandbergen, H. W. *Mater. Sci. Eng., A* **2005**, *390*, 127−138.

(3) Vissers, R.; van Huis, M. A.; Jansen, J.; Zandbergen, H. W.; Marioara, C. D.; Andersen, S. J. *Acta Mater.* **2007**, *55*, 3815−3823.

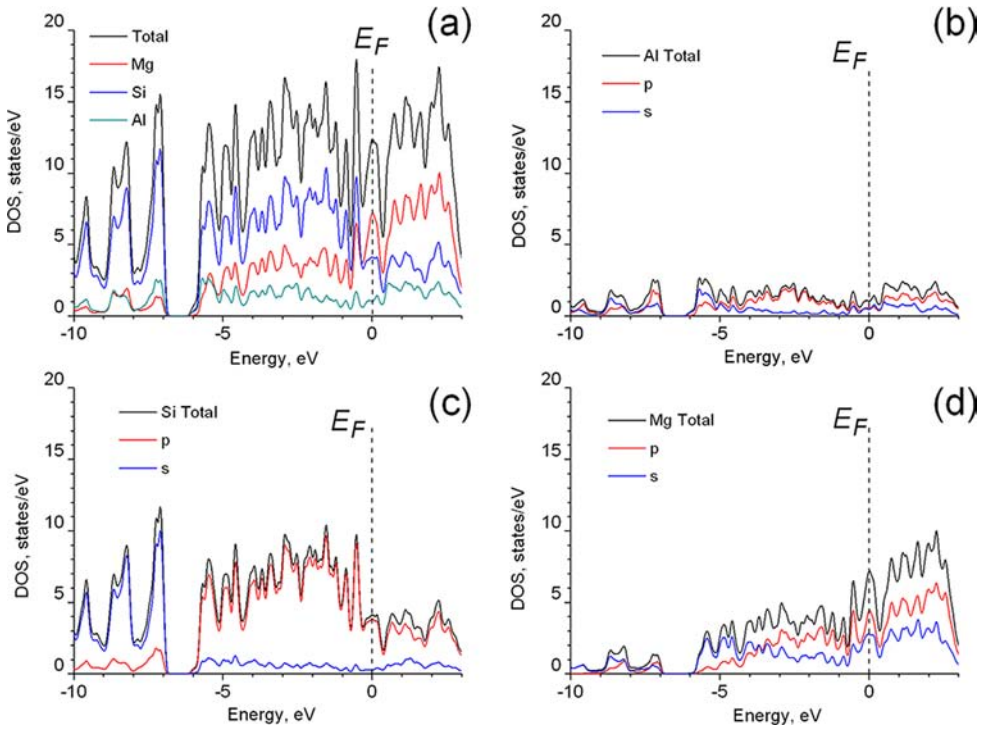

Figure 10. Electron density of states (DOS) for Mg_4AlSi_3 calculated using CASTEP software: (a) total DOS for Mg_4AlSi_3, partial DOS for (b) Al, (c) Si, and (d) Mg.

dx.doi.org/10.1021/ic3027539 | *Inorg. Chem.* 2013, 52, 3953−3961

(4) Andersen, S. J.; Marioara, C. D.; Vissers, R.; Froseth, A.; Zandbergen, H. W. *Mater. Sci. Eng., A* **2007**, *444*, 157−169.
(5) *Ternary Alloys, A Comprehensive Compendium of Evaluated Constitutional Data and Phase Diagrams*; Chakraborti, N., Lukas, H. L., Bodak, O., Rokhlin, L., Effenberg, G., Aldinger, F., Rokhkin, L., Eds.; Materials Science International Services GmbH: Stuttgart, 1999; Vol. *16*, pp 382−398.
(6) Nikitin, E. N.; Tkalenko, E. N.; Zaitsev, V. K.; Zaslavskii, A. I.; Kuznetsov, A. K. *Neorg. Mater.* **1968**, *4*, 1902−1906.
(7) Hao, J.; Zou, B.; Zhu, P. W.; Gao, C. X.; Li, Y. W.; Liu, D.; Wang, K.; Lei, W. W.; Cui, Q. L.; Zou, G. T. *Solid State Commun.* **2009**, *149*, 689−692.
(8) Yu, F.; Sun, J. X.; Yang, W.; Tian, R. G.; Ji, G. F. *Solid State Commun.* **2010**, *150*, 620−624.
(9) Kawai, N.; Endo, S. *Rev. Sci. Instrum.* **1970**, *41*, 1178−1181.
(10) Sheldrick, G. *Acta Crystallogr.* **2008**, *64*, 112−122.
(11) Farrugia, L. *J. Appl. Crystallogr.* **1999**, *32*, 837−838.
(12) Clark, S. J.; Segall, M. D.; Pickard, C. J.; Hasnip, P. J.; Probert, M. J.; Refson, K.; Payne, M. C. *Z. Kristallogr.* **2005**, *220*, 567−570.
(13) CASTEP is available from Accelrys, San Diego, CA, http://www.accelrys.com.
(14) Yan, X.-Y.; Zhang, F.; Chang, Y. A. *J. Phase Equilib.* **2000**, *21*, 379−384.
(15) Bolotina, N. B.; Dyuzheva, T. I.; Bendeliani, N. A.; Petricek, V.; Petrova, A. E.; Simonov, V. I. *J. Alloys Compd.* **1998**, *278*, 29−33.
(16) Remschnig, K.; Le Bihan, T.; Noel, H.; Rogl, P. *J. Solid State Chem.* **1992**, *97*, 391−399.
(17) Steinberg, G.; Schuster, H.-U. *Z. Naturforsch.* **1979**, *34b*, 1237−1239.
(18) Lukachuk, M. y.; Pottgen, R. *Z. Kristallogr.* **2003**, *218*, 767−787.
(19) Mulliken, R. S. *J. Chem. Phys.* **1955**, *23*, 1833−1840.
(20) Segall, M. D.; Pickard, C. J.; Shah, R.; Payne, M. C. *Mol. Phys.* **1996**, *89*, 571−577.
(21) Segall, M. D.; Shah, R.; Pickard, C. J.; Payne, M. C. *Phys. Rev. B* **1996**, *54*, 16317−16320.